

Supplementary Materials

Microwave-assisted synthesis of nitrogen doped carbon dots using prickly pear as the carbon source and its application as highly selective sensor for Cr(VI) and as patterning agent

Shreya Bhatt^{a,b}, Gaurav Vyas^{a,b} and Parimal Paul^{a,b,*}

^aAnalytical and Environmental Science Division & Centralized Instrument Facility, CSIR-Central Salt and Marine Chemicals Research Institute, G. B. Marg, Bhavnagar 364002, India.

^bAcademy of Scientific and Innovative Research (AcSIR), Ghaziabad- 201002, India.

* Corresponding author: ppaul@csmcri.res.in.

List of Supplementary Materials

Figure/ Table No.	Figure/Table caption	Page No.
Table S1	Quantum yield calculation of N-CDs.	2
Table S2	Fluorescence lifetime data with bi-exponential fit of the fluorescence decay curves of N-CDs and NCDs+Cr(VI).	3
Table S3	Different parameters for analysis of real sample using Stern-Volmer equation.	4
Fig. S1	Raman spectrum of N-CDs.	5
Fig. S2	Fluorescence decay curve of N-CDs recorded at 360 nm excitation.	6
Fig. S3	Bar diagram showing change in fluorescence intensity of N-CDs at different pH ranging from 2 to 12. ($\lambda_{\text{ex}} = 360 \text{ nm}$, $\lambda_{\text{emi}} = 450 \text{ nm}$). (Red marking with metal ion).	7
Fig. S4	Fluorescence spectra of N-CDs with 0.5 to 5.0 % of NaCl is shown. The intensity of the fluorescence band as a function of concentration of NaCl is shown in the inset.	8
Fig. S5	Plot of the change in fluorescence intensity of N-CDs in presence of different concentrations of Cr(VI) as a function of time (0 to 60 min).	9
Fig. S6	Fluorescence spectral change of N-CDs in presence of various metal ions ($\lambda_{\text{ex}} = 360 \text{ nm}$).	10
Fig. S7	Fluorescence decay curve of N-CDs in presence of Cr(VI).	11

Table S1. Quantum yield calculation of N-CDs.

Sample name	Integrated emission intensity (I)	Absorbance (A) at 360 nm	Refractive index of solvent (η)	Quantum yield (Q) at 360 nm
Quinine sulphate	542308	0.132	1.33	0.54 (known standard value)
N-CDs	80758	0.0752	1.33	0.148

Table S2. Fluorescence lifetime data with bi-exponential fit of the fluorescence decay curves of N-CDs and NCDs+Cr(VI).

Sample	τ_1/ns (%)	τ_2/ns (%)	$\tau_{\text{ave}}/\text{ns}$
N-CDs	1.46 (47)	8.10 (53)	4.979
N-CDs + Cr(VI)	1.40 (44)	7.56 (56)	4.849

Table S3. Different parameters for analysis of real sample using Stern-Volmer equation.

Sample No.	Spiked (μM)	Intensity (I ₀)(a.u)	Intensity of Sample (I) (a.u)	I ₀ /I (a.u)	Calculated Concentration (μM)
DW-1	15	3.9745	2.89	1.373	15.1
DW-2	30	3.9745	2.23	1.786	31.8
TW-1	25	3.9745	2.45	1.625	25.8
TW-2	35	3.9745	2.05	1.936	37.8

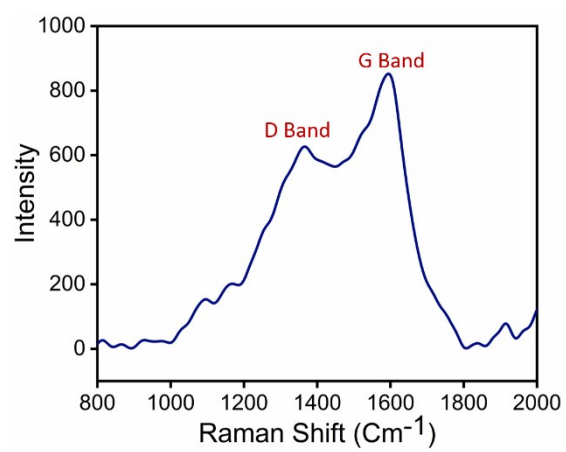


Fig. S1. Raman spectrum of N-CDs.

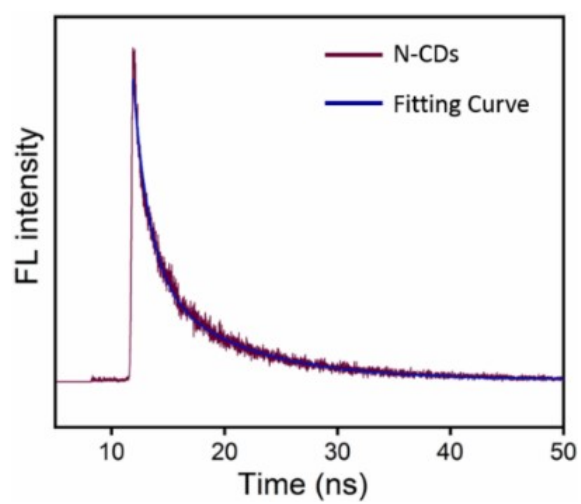


Fig. S2. Fluorescence decay curve of N-CDs recorded at 360 nm excitation.

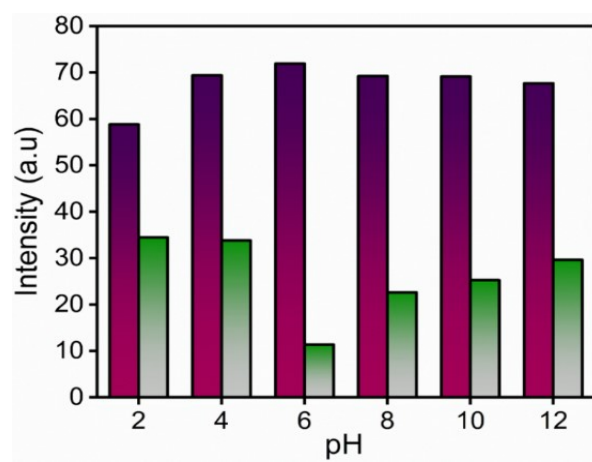


Fig. S3. Bar diagram showing change in fluorescence intensity of N-CDs at different pH ranging from 2 to 12. ($\lambda_{ex} = 360 \text{ nm}$, $\lambda_{emi} = 450 \text{ nm}$). (Red marking with metal ion).

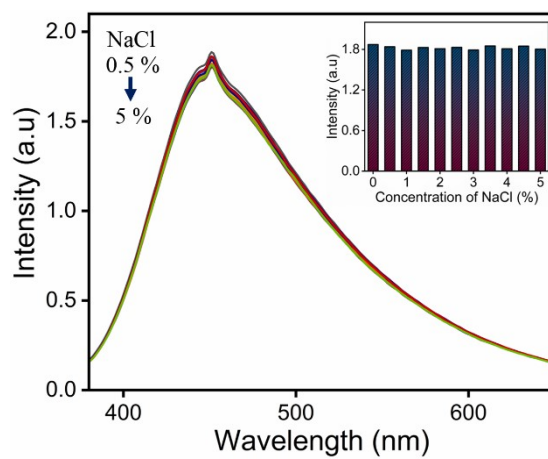


Fig. S4. Fluorescence spectra of N-CDs with 0.5 to 5.0 % of NaCl is shown. The intensity of the fluorescence band as a function of concentration of NaCl is shown in the inset.

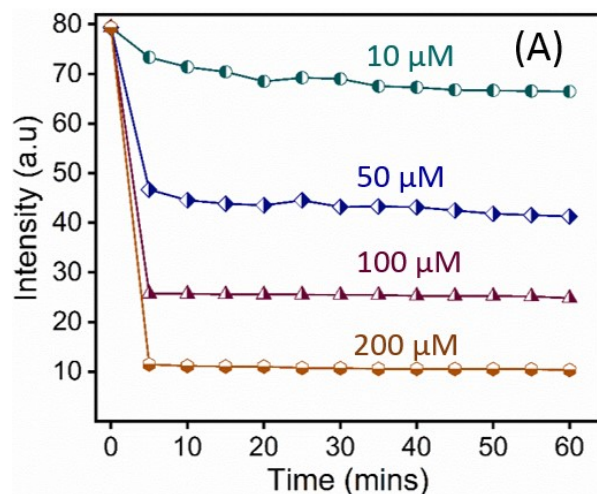


Fig. S5. Plot of the change in fluorescence intensity of N-CDs in presence of different concentrations of Cr(VI) as a function of time (0 to 60 min).

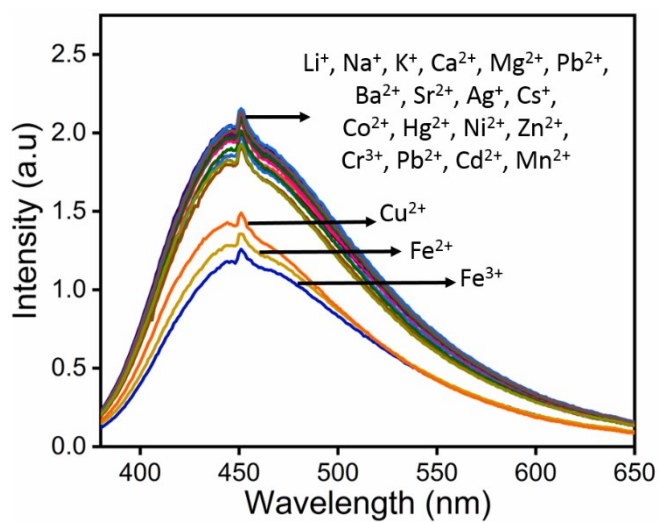


Fig. S6. Fluorescence spectral change of N-CDs in presence of various metal ions ($\lambda_{\text{ex}} = 360$ nm).

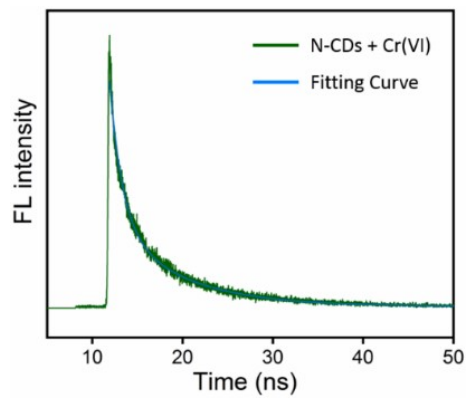


Fig. S7. Fluorescence decay curve of N-CDs in presence of Cr(VI).